



## EVALUATION OF THE COMPRESSION BEHAVIOUR OF CONFINED BOUNDARY ELEMENTS IN DUCTILE REINFORCED CONCRETE BLOCK MASONRY STRUCTURAL WALLS

Ala' Obaidat

PhD Candidate, Department of Building, Civil and Environmental Engineering, Concordia University, Montréal, Québec, Canada

[atobaidat@yahoo.com](mailto:atobaidat@yahoo.com)

Ahmad Abo El Ezz

Postdoctoral Fellow, Department of Building, Civil and Environmental Engineering, Concordia University, Montréal, Québec, Canada

[aboeezz@gmail.com](mailto:aboeezz@gmail.com)

Khaled Galal

Professor, Department of Building, Civil and Environmental Engineering, Concordia University, Montréal, Québec, Canada

[galal@bcee.concordia.ca](mailto:galal@bcee.concordia.ca)

**ABSTRACT:** Reinforced concrete masonry structural walls are commonly used as lateral force resisting systems for existing buildings in seismic regions. Recent North American code provisions for seismic design of masonry structures introduced the use of special reinforced concrete masonry structural wall systems with column-like boundary elements for improved ductile performance under severe ground motion levels. The characterisation of the compression behaviour of the boundary elements is essential for the reliable evaluation of the ductility capacity of walls. This paper presents an experimental investigation on the compression stress-strain behaviour of pilaster block reinforced boundary elements. Seventeen full-scale pilaster block boundary elements were tested under concentric axial compression load. Confinement of the grouted core is provided by transverse reinforcement in the form of seismic hoops with different diameters and spacing. The influence of different configurations of the confinement reinforcement on the compression strain ductility is presented. The results showed that the confinement reinforcement increased the strength by the range of 1.2 to 1.3 times the strength of the unreinforced elements. On the other hand, confinement increased the ultimate strain capacity at 50% strength degradation by the range of 1.52 to 3.37 times of the unreinforced boundary elements. The results of this testing program are particularly useful for the evaluation of the ductility capacity of reinforced masonry walls with boundary elements.

Keywords: Reinforced Masonry walls; Boundary elements; Confinement; stress-strain.

**Introduction** Reinforced concrete masonry structural walls are commonly used as lateral force resisting systems for existing buildings in seismic regions. In regions of moderate to high seismicity, reinforced masonry walls are expected to undergo inelastic response during severe ground motions. Therefore, special considerations must be given to detailing of the horizontal and vertical reinforcement, especially at the ends of such walls in order to resist the high curvature ductility demands. Confinement of the wall end section is an efficient approach to enhance the curvature ductility capacity in reinforced masonry walls. A key component in the evaluation of the ductility capacity of reinforced masonry walls is the evaluation of compression stress-strain behaviour of the confined ends. Figure 1 shows some of the previously proposed methods to enhance the strain ductility capacity at the walls end zones including adding steel

plates or confinement combs at mortar joints, spiral ties reinforcement of the grouted cores and adding a column-like boundary element with confinement hoops. Priestley and Elder (1983) investigated the improvement of the ultimate compression strain and the post-peak branch characteristics of the concrete masonry prisms that were confined by steel plates at mortar joints. The researchers concluded that the confinement steel plates improved the ductility of the concrete masonry prisms. Hart et al (1988) studied different configurations of confinement reinforcement steel in concrete masonry prisms including; modified Priestley plates, open wire mesh (seismic combs), closed wire mesh, steel ring cages and spirals cages. The researchers concluded that the confinement had limited effect on the ascending approach and had a positive effect on the descending post-peak stress strain portion by decreasing the slope (improved strain ductility). Dhanasekar and Shrive (2002) examined the effectiveness of using rolled wire mesh to confine the grouted cells in unreinforced concrete block prisms. The researchers concluded that the confinement resulted in better post-peak behaviour of stress strain curve and increased the ultimate strain. Malmquist, K. J. (2004) constructed and tested forty-five concrete block prisms confined by steel plates and combs. The researcher found that the confinement exhibited more strain at 50% strength degradation and produced more softening compared to an unconfined prism. More recently, Shedid et al. (2010); Banting and El-Dakhakhni (2012) studied the effect of adding boundary elements on the RM wall behaviour. The researchers concluded that adding boundary element delay the buckling of reinforcement bars, added out of plane stability and hence limited the damage of the end wall (toe), and increased the displacement ductility and drift capacity.

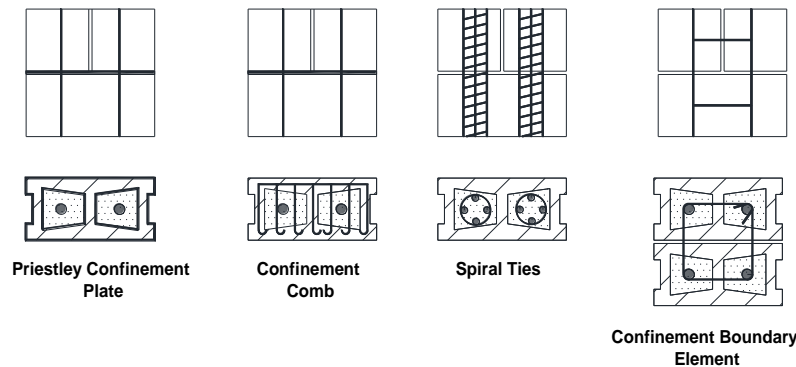


**Figure 1 – Examples of different confinement methods of reinforced masonry walls including boundary element (Adapted from Banting, 2013).**

Recent codes for the Design of Masonry Structure including the Canadian Code (CSA S304-14, 2014) and the American Code, Masonry Standards Joint Committee (MSJC, 2013) are introducing the use of Ductile Reinforced Masonry structural Walls with column-like boundary elements for the improvement of the ductility capacity of the walls. However, limited research was conducted to evaluate the detailing requirements for the confined boundary elements (Abo El Ezz et al. 2015). Hence, there is a need for experimental and analytical studies to investigate the influence of confinement reinforcement and detailing on the compression stress-strain behaviour of the boundary elements. This paper presents an experimental investigation on the compression stress-strain behaviour of unconfined and confined reinforced boundary element columns constructed from concrete pilaster blocks. The investigated columns are representative of the highly compressed end zones of a reinforced masonry structural wall. The influence of different configurations of confinement reinforcement is investigated.

## Experimental Program

A total of 17 full-scale fully grouted concrete Pilaster masonry boundary element columns were constructed and tested. The horizontal reinforcement in the form of seismic hoops has been placed prior to the pilaster blocks construction. The boundary element columns were constructed with the help of certified masons. Pilaster blocks (190mm depth x 190mm width x 390 mm length) with compressive strength of 15 MPa was used in the boundary elements construction. Typical dimensions of the unreinforced boundary element columns are shown in Figure 2. Each boundary element column consisted of five block layers placed on concrete footing with dimension [400mm length x 400mm width x 250mm depth]. Each course of the boundary elements was made of two block units placed together in

alternating directions along the height of boundary element with across sectional size of 390mm x 390 mm as drawn in Figure 2. The blocks were joined together with 10mm mortar joints. The reinforced boundary elements contained two layers of vertical reinforcement bars with two bars each of 20M [ $A_{sv}=300 \text{ mm}^2$ ] (four bars in total), vertical reinforcement ran continuously from the base of footing to over the height of boundary element without lap splices. Square-shaped hoops with outer dimensions of 250mmx250mm with different diameters were placed at vertical spacing as shown in test matrix Table 1. Figure 2 shows the construction details of all configurations for the reinforced confined boundary element columns. Figure 3 shows the sequence of the placement of the ties and blocks of the boundary element. The boundary elements were filled by standard grout mixed at the lab, the grout was consolidated by rodding in three divisions and dry stone was casted at the top and bottom of the test units in order to provide a smooth surface for testing. The confinement ratio  $C_f$  is calculated using Eq. 1. as shown in Table 1, where  $\rho_s$  is the volumetric ratio of the confinement reinforcement (the volume of confinement hoops to the volume of core concrete at spacing  $S$ );  $H$  is the width of the confined core (250mm in this case) and  $S$  is the spacing between the confinement seismic hoops.

$$C_f = \rho_s \sqrt{(H/S)} \tag{1}$$

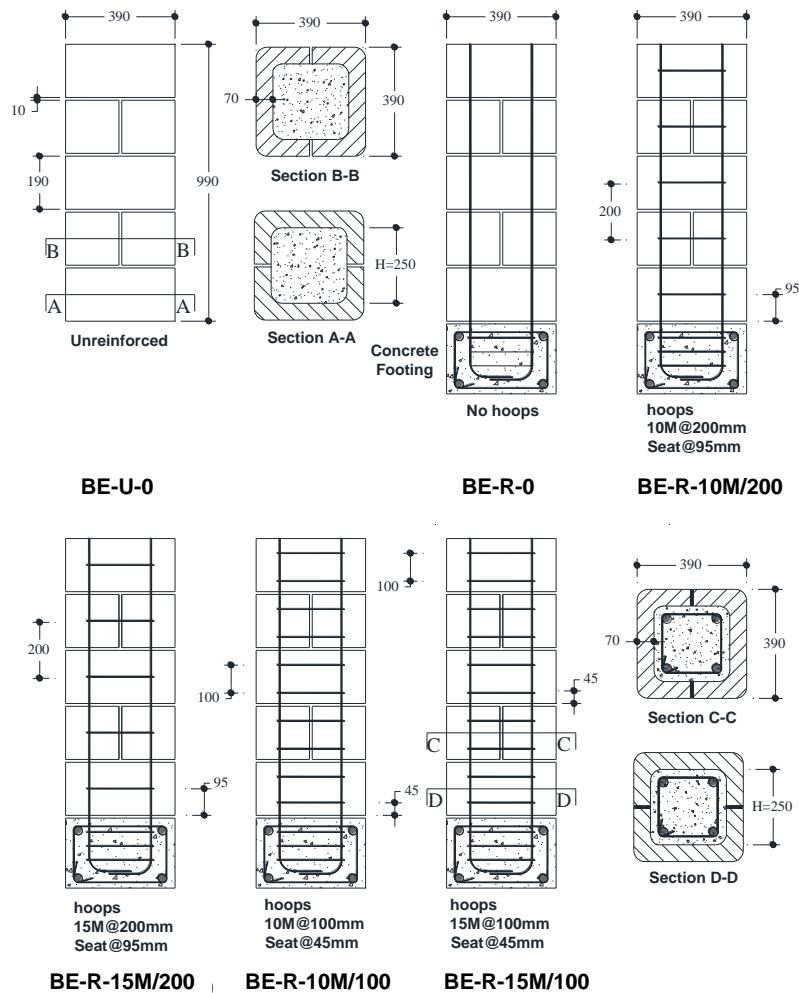
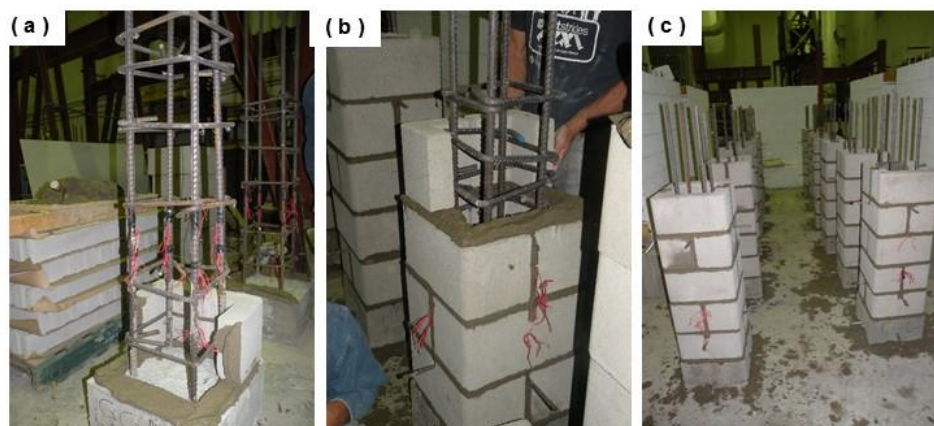


Figure 2– Construction Details of unreinforced and reinforced concrete pilaster block masonry boundary elements.

**Table 1: Test matrix of concrete Pilaster block masonry boundary elements.**

Boundary element ID	Number of tested units	Vertical reinforcement	Transverse reinforcement (hoops)	Volumetric ratio of (hoops) $\rho_s$ %	Confinement ratio $C_f$
BE-U-0	2	-	-	0	0
BE-R-0	3	4-20M	-	0	0
BE-R-10/200	3	4-20M	10M@200mm	0.0080	0.0088
BE-R-15/200	3	4-20M	15M@200mm	0.0152	0.0170
BE-R-10/100	3	4-20M	10M@100mm	0.0157	0.0248
BE-R-15/100	3	4-20M	15M@100mm	0.0314	0.0497



**Figure 3—The construction sequence of the concrete pilaster blocks: (a), (b) Illustration of the placement of the blocks in the masonry boundary element (c) the boundary elements after Pilaster blocks construction.**

### Material Properties

The materials used for construction of the pilaster block boundary elements are summarized in Table 2. A 70 mm thickness of full scale of the Pilaster block (190mm depth x 190mm width x 390mm length) was used in the construction of the test boundary elements specimens using Type S-mortar between the different courses with average thickness of 10mm as shown in Figure 3. The Type S-Mortar prepared according to CSA A179. Coarse grout mixed at the lab was used. Reinforcement steel with yield strength 420MPa (CSA G30.18-09, 2009) was used in boundary element construction. The stress strain curves of three different diameters are shown in Figure 4.

Table 2. Properties of materials used in the construction of the boundary elements.

Material	Property	Value	C.O.V %
Concrete	$f'_c$ (MPa)	35	6.5
Masonry block	$f'_c$ (MPa)	15	3.5
Mortar <sup>a</sup>	$f'_{mr}$ (MPa)	13	10
grout <sup>a</sup>	$f'_g$ (MPa)	35	6.5
Reinforcement steel	$f_y$ (MPa)	420	7.5

<sup>a</sup>28-30 days strength; 1MPa=145psi  
C.O.V (coefficient of variation)

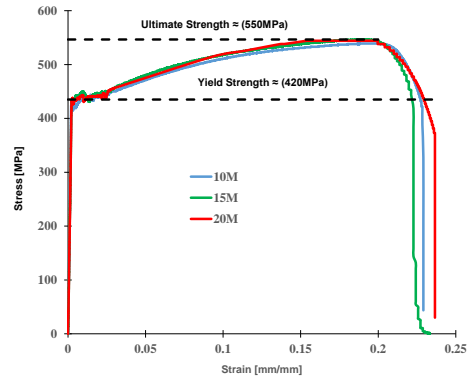


**Figure 4– Stress-strain curves for the reinforcement steel used in the construction of the boundary elements.**

### Test setup and instrumentation

The concrete Pilaster masonry boundary element columns were tested in compression using (12MN) MTS machine at Ecole Polytechnique de Montreal as shown in Figure 5. The tests were conducted in a displacement control mode in order to capture the post-peak behaviour, hence, quantify the influence of the confinement reinforcement on the post-peak stress-strain behaviour. The test setup consisted of; the MTS machine a steel frame transfer load to the strong floor; a 12MN hydraulic cylinder; 50mm perforated rigid rectangular steel plate for transfer a uniformly distributed load to the test unit and strong floor supporting the test unit. The vertical displacement of the boundary element columns was measured using four cable-extension transducers (potentiometers) LVDT's attached at the centerline of the sides of the unit that glued underneath bearing plate and at the top of footing. The gauge length for the potentiometers was 1020 mm measuring between bearing plate to the top of concrete footing.

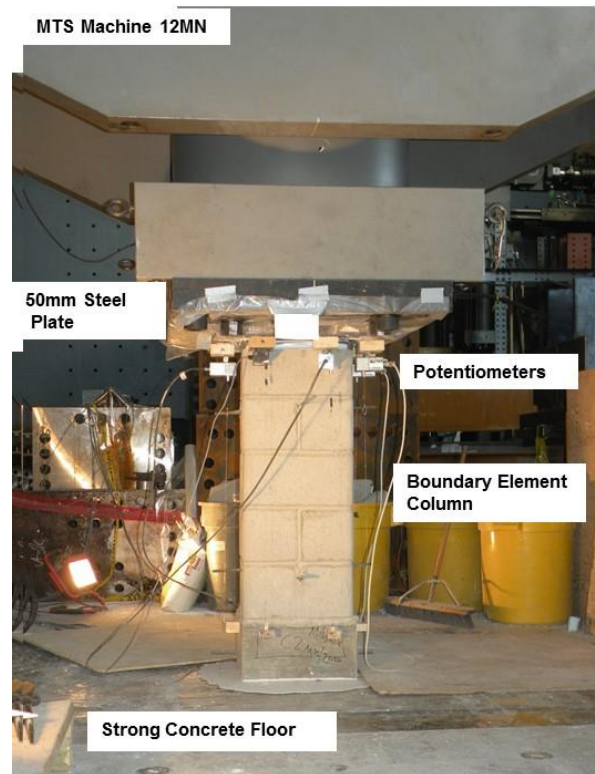


**Figure 5–Photograph illustration of the MTS testing Machine and the loading system.**

## Test Results

Figure 6 shows the observed average compressive stress strain for all masonry boundary elements test units including unreinforced, unconfined reinforced and reinforced confined boundary elements. It can be observed that the confinement horizontal reinforcement (hoops) produced more gradual post-peak stress-strain behavior and improved the strain ductility of the boundary element with the increase of the confinement ratio. The increase of the strength was in the range of 1.2 to 1.3, however, the increase of the strain at 75% strength degradation was in range of 1.35 to 1.63 and the increase of the the strain at 50% strength degradation was in range of 1.52 to 3.37 times of the unreinforced units.

### Test observations:

The unreinforced boundary elements (Units BE-U-0): The average observed stress-strain relationship for (test units BE-U-0) is presented in Figure 7. Figure 7 shows the damage conditions of the unreinforced boundary element column. The damage sequence of the unreinforced units was as follows: visible vertical splitting cracks along the face shells at peak load, spalling of the face shells, grouted core crushing. A sudden drop of the load was observed after peak load with extensive crushing of the grouted core.

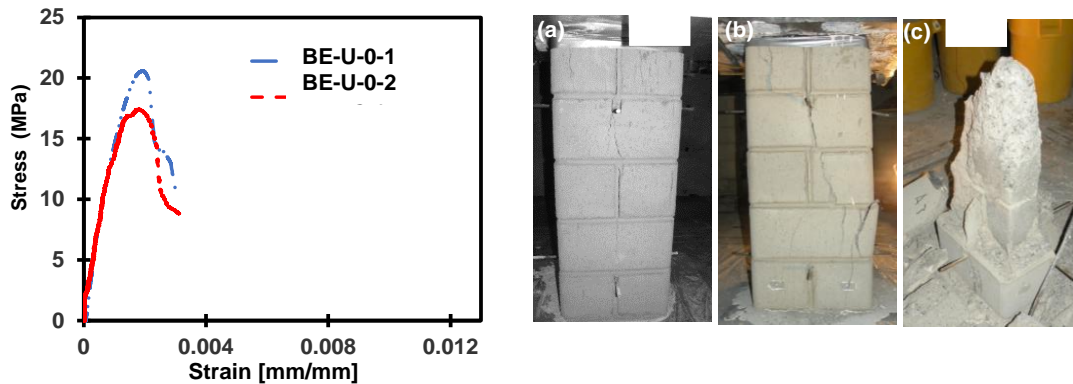


Figure 7–Observed stress-strain curves and failure mechanism of the unreinforced boundary elements.

Table 3 shows the results of the maximum observed stress  $f_{max}$ , strain at maximum stress  $\epsilon_{max}$ , strain at 75% strength degradation  $\epsilon_{75}$  and the ultimate strain at 50% strength degradation  $\epsilon_{50}$ . Observations were made based on the obtained stress strain behaviour of the reinforced boundary elements as discussed in the following section

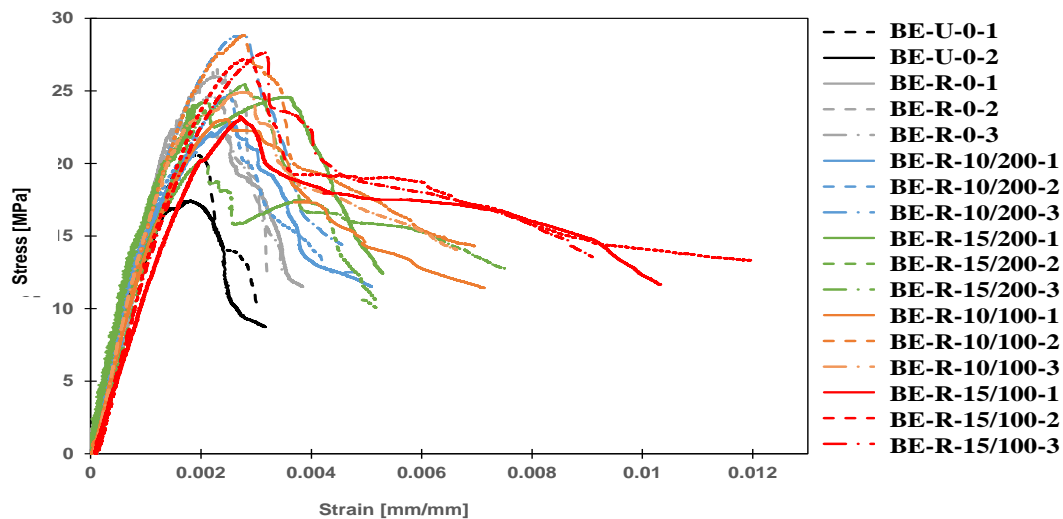
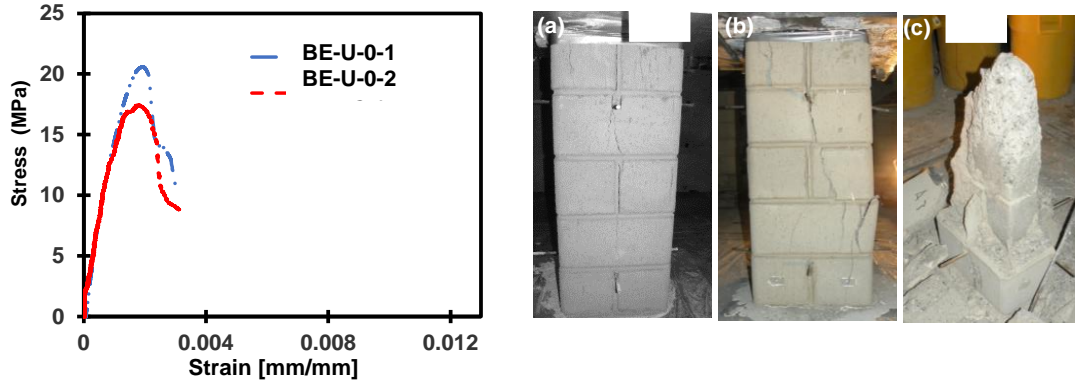


Figure 6–Observed stress–strain curves for all test units including unreinforced, unconfined reinforced and reinforced confined boundary elements

**Test observations:**

The unreinforced boundary elements (Units BE-U-0): The average observed stress-strain relationship for (test units BE-U-0) is presented in Figure 7. Figure 7 shows the damage conditions of the unreinforced boundary element column. The damage sequence of the unreinforced units was as follows: visible vertical splitting cracks along the face shells at peak load, spalling of the face shells, grouted core crushing. A sudden drop of the load was observed after peak load with extensive crushing of the grouted core.



**Figure 7–Observed stress-strain curves and failure mechanism of the unreinforced boundary elements.**

**Table 3: Results for the reinforced units for maximum observed stress, maximum strain, strains at 75% and 50% strength degradation.**

Test unit	Maximum Stress $f_{max}$ [MPa]		Maximum strain $\epsilon_{max}$ [mm/mm]		Strain at 75% strength degradation $\epsilon_{75}$ [mm/mm]		Ultimate strain at 50% strength degradation $\epsilon_{50}$ [mm/mm]	
	Observed	Average and COV(%)	Observed	Average And COV(%)	Observed	Average and COV(%)	Observed	Average And COV(%)
BE-U-0-1	20.6	18.95 (12%)	0.002	0.0019 (7%)	0.0024	0.00245 (3%)	0.003	0.0031 (5%)
BE-U-0-2	17.25		0.0018		0.0025		0.0032	
BE-R-0-1	21.8	24.13 (9%)	0.002	0.00223 (11%)	0.0031	0.0029 (7%)	0.0037	0.0035 (7%)
BE-R-0-2	26		0.0025		0.0028		0.0032	
BE-R-0-3	24.6		0.002		0.0027		0.0035	
BE-R-10/200	22.8	25.36 (12%)	0.0025	0.00256 (4%)	0.0034	0.0033 (5%)	0.005	0.0047 (5%)
BE-R-10/200	24.6		0.0025		0.0031		0.0047	
BE-R-10/200	28.7		0.0027		0.0034		0.0045	
BE-R-15/200	24.6	23.44 (12%)	0.0022	0.00233 (14%)	0.0042	0.004 (11%)	0.0053	0.006 (22%)
BE-R-15/200	20.32		0.0021		0.0043		0.0051	
BE-R-15/200	25.4		0.0027		0.0035		0.0075	
BE-R-10/100	23	25.5 (11%)	0.0025	0.00263 (5%)	0.0037	0.0036 (3%)	0.007	0.00683 (3%)
BE-R-10/100	28.5		0.00275		0.0035		0.0069	
BE-R-10/100	25		0.00265		0.0036		0.0066	
BE-R-15/100	23	25.83 (10%)	0.0027	0.003 (11%)	0.0041	0.00386 (8%)	0.0103	0.0104 (14%)
BE-R-15/100	27		0.00278		0.0035		0.012	
BE-R-15/100	27.5		0.0033		0.004		0.009	

**Test units BE-R-0:** Figure 8 shows the stress-strain curves of the test units and damage mechanisms. The test units exhibited 1.2 times increase in the strength compared to the BE-U-0 unit due to the presence of the vertical bars. The damage mechanisms of the units were as follows: vertical splitting cracks were observed at peak loads followed by spalling of the of the face shells and simultaneous core crushing and vertical bar buckling. The post-peak behaviour was similar to the unreinforced units with a steep slope observed after peak load.

**Test units BE-R-10/200 and BE-R-15/200:** Test units BE-R-10/200 and BE-R-15/200, confined by hoops 10M/200 mm and 15M/200, respectively, along with the vertical reinforcement to evaluate the effect of confinement on the behaviour of compression stress strain curve. It can be observed that the test units exhibited slight increase in strength of 1.02 times compare to the vertically reinforced units. However, more gradual post-peak behaviour was observed due to the presence of confinement hoops. The ultimate strain and strain at 50% strength degradation are 1.52 and 1.75 times, respectively, of corresponding strain in (BE-U-0).The damage mechanisms of the units were as follows: vertical splitting cracks at peak load followed by spalling of the face-shells and simultaneous core crushing and buckling of the vertical bars (Figure 9).

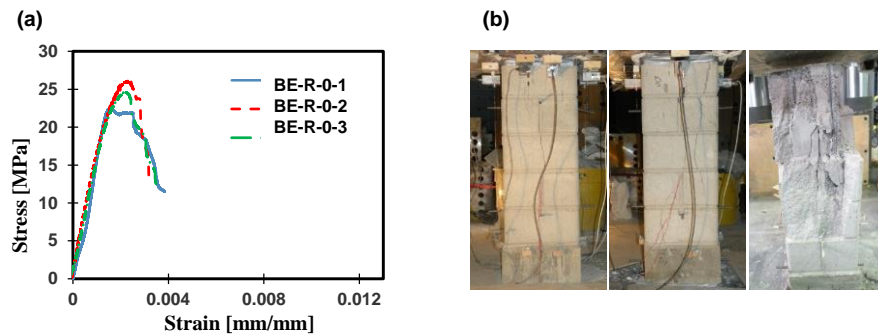


**Figure 8—Observed stress-strain curves and failure mechanism of the vertically reinforced boundary elements**

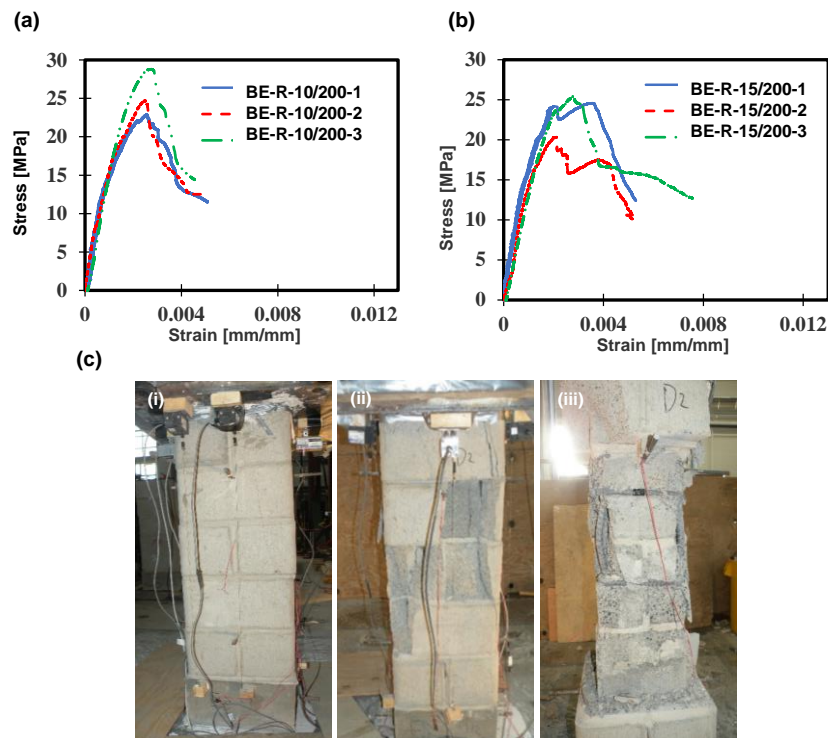


**Figure 9—Observed stress-strain curves and failure mechanism for boundary elements (BE-R-10/200 and BE-R-15/200).**

**Test units BE-R-10/100 and BE-R-15/100:** Test units BE-R-10/100 and BE-R-15/100 exhibited milder post-peak strain softening behaviour compared to test units BE-R-10/200 and BE-R-15/200 due to the presence of higher confinement ratio as show in Figure 10-a and Figure 10-b. After peak load, a 25% drop in the load was observed followed by a mild post-peak slope. This is mainly attributed to the cracking and spalling of a significant portion of the cross-sectional area (the face-shells represent 50% of the total area) and the difference in the compression strength of the face-shells (15MPa) and the grouted core (35MPa). The mechanism failures are similar to the units BE-R-10/200 and BE-R-15/200, however, rupture of some hoops was observed in BE-R-15/100-2 test unit (Figure 10-c). The strain ductility increased due to the closer spacing of the confinement transverse reinforcement (100mm) instead of (200mm).

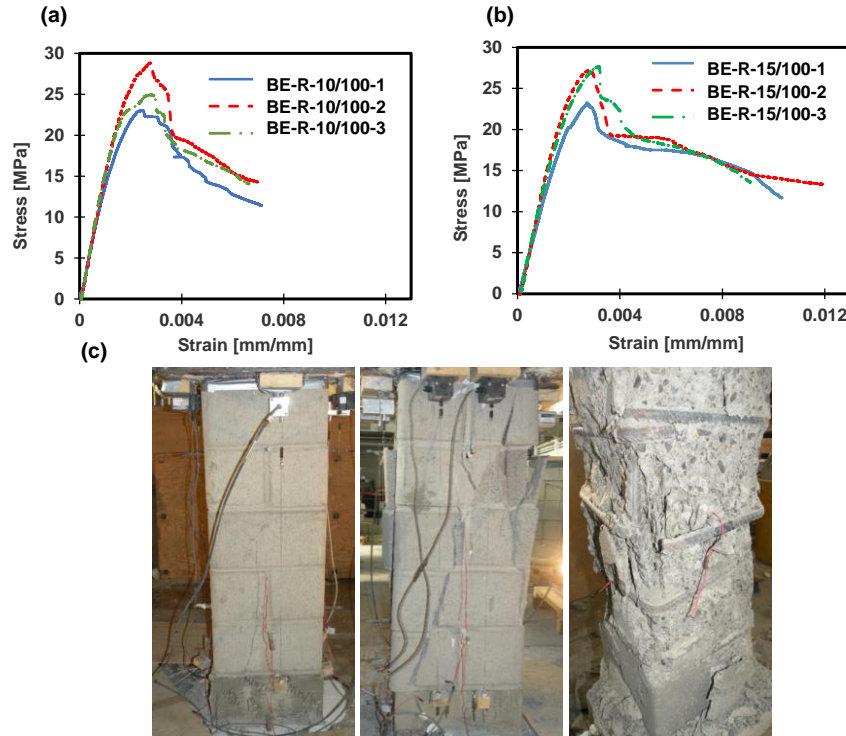


**Figure 10—Observed stress-strain curves and failure mechanism for boundary elements (BE-R-10/100 and BE-R-15/100).**

### Effect of confinement ratio

Figure 11 shows the correlation between the confinement ratio and the ratio of maximum strength of the confined units and strength of unreinforced unit. The  $f_{max-C}$  is the average strength of the confined boundary element;  $f_{max-U}$  is the average strength of the unreinforced boundary element. It can be observed that the reinforced and confined units exhibited an increase in the strength in the range of 1.1 to 1.4 times the strength of the unreinforced units. On other hand, the increase in the confinement ratio provided more strain ductility and has a significant effect on the post-peak behaviour with softening of the descending branch of the stress-strain curve as shown in the previous section. The maximum dependable masonry compression strain in this study was at 50% strength degradation varied between 0.0047 to 0.0104. Hart et al (1988) defined the design strength limit state when the strength has reduced by 50% from its maximum value (i.e., the design strain at 50% strength degradation), the strain at 50% degradation was 0.004 for confinement masonry prism. Ewing and Kowalsky (2004) reported the Maximum dependable masonry compression strain, occurring at 50% strength degradation. This limit state values for both masonry alternate course confined and every course confined were 0.015 and 0.0344, respectively. Figure 12 shows the correlation between the confinement ratio ( $C_f$ ) and the dependable compressive strain corresponding to 50% ( $\epsilon_{50}$ ) strength degradation.

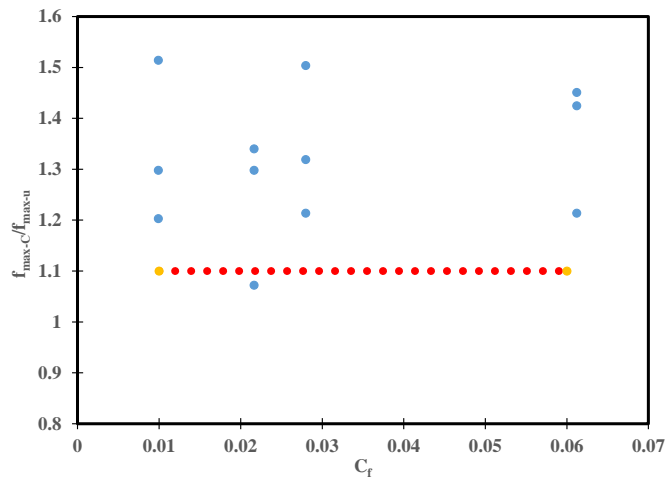


**Figure 11—Correlation between the strength enhancement ratio and the confinement ratio based on test results.**

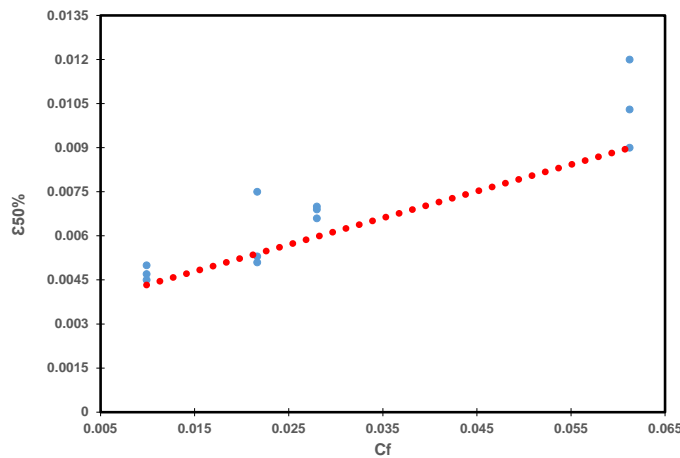


**Figure 12—Correlation between the strain at 50% strength degradation and the confinement ratio based on test results.**

### Conclusions and future research

This paper presented the results of an experimental investigation for the evaluation of the compression stress-strain behaviour of reinforced concrete block boundary elements. Confinement of the grouted core is provided by transverse reinforcement in the form of seismic hoops with different diameters and spacing. The influence of different configurations of the confinement reinforcement on the compression strain ductility was presented. Seventeen full-scale pilaster block boundary elements were tested under concentric axial compression load including unreinforced and reinforced units. The results showed that the confinement reinforcement increase the strength by the range 1.2 to 1.3 of the unreinforced boundary elements, however, increase the ductility capacity by the range 1.52 to 3.37 times of the unreinforced units boundary elements. In addition, improved the softening of the post-peak behaviour compared to the unreinforced units. The results of this testing program are particularly useful for the evaluation ductility capacity of reinforced masonry walls with boundary elements. It should be noted that observations from testing program are limited to one combination of face-shell strength, grout strength and steel yield strength parameters. Different combinations of these parameters need to be investigated to provide recommendations for the strain capacities for ductile design of structural walls with boundary elements.

## Acknowledgments:

This study was supported by the Natural Science and Engineering Research Council of Canada (NSERC) and was conducted in collaboration with the Canada Masonry Design Centre (CMDCC) and the Canadian Concrete Masonry Producers Association (CCMPA). The authors would like to acknowledge the help of the technical staff at Ecole Polytechnique Montreal during the testing program.

## References

- Abo El Ezz, A., Seif Eldin, H. M., and Galal, K. (2015). "Influence of confinement reinforcement on the compression stress-strain of grouted reinforced concrete block masonry boundary elements." *Journal of Structures*.
- Banting, B.R. and El-Dakhkhni, W.W. (2012). "Force- and Displacement-Based Seismic Performance Parameters for Reinforced Masonry Structural Walls with Boundary Elements." *Journal of Structural Engineering*, February 2012.
- CSA A179. (2004). Mortar and grout for unit masonry, CSA, Mississauga, ON, Canada.
- CSA G30.18-09. (2009). Carbon steel bars for concrete reinforcement. Canadian Standards Association, Mississauga, Ontario, Canada.
- CSA S304-14. Design of masonry structures. Mississauga, Ontario, Canada: Canadian Standards Association; 2014.
- Dhanasekar, M. and Shrive, N. G. (2002). "Strength and Deformation of Confined and Unconfined Grouted Concrete Masonry." *ACI Structural Journal*, 99(6), p.819-826.
- Ewing and Kowalsky (2004). "The Compressive Behavior of Unconfined and Confined Clay Brick Masonry." *Journal of Structural Engineering*, Vol. 130, No. 4, pp 650-661.
- Hart, G., Noland, J., Kingsley, G., Englekirk, R., and Sajjad, N. A. (1988). "The Use of Confinement Steel to Increase the Ductility in Reinforced Concrete Masonry Shear Walls." *Masonry Society Journal*, Vol. 7, No.2, T19I-42.
- Malmquist, K. J. (2004). "Influence of confinement reinforcement on the compressive behavior of concrete block masonry and clay brick masonry prisms." Special Report, Washington State University, Washington, USA.
- Masonry Standards Joint Committee (MSJC). (2011). Building Code Requirements for Masonry Structures." TMS 402/ACI 530/ASCE 5, American Concrete Institute, Farmington Hills, MI., American Society of Civil Engineers, Reston, VA and The Masonry Society, Boulder, CO.
- Priestley, M.J.N., and Elder, D.M. (1983). "Stress-Strain Curves for Unconfined and Confines Concrete Masonry." *ACI Journal*. Vol. 80, No. 3, pp 192-201.
- Shedid, M.T., El-Dakhkhni, W.W. and Drysdale, R.G. (2010). "Alternative Strategies to Enhance the Seismic Performance of Reinforced Concrete-Block Shear Wall Systems." *Journal of Structural Engineering*, 136(6), 676-689.